Journal of Water Process Engineering 36 (2020) 101257

Contents lists available at ScienceDirect

Journal of Water Process Engineering

journal homepage: www.elsevier.com/locate/jwpe

Gravity-driven membrane (GDM) filtration of algae-polluted surface water

Lars Truttmann[a,b,1], Yixi Su[c,1], Seonki Lee[d,1], Michael Burkhardt[b], Sigurður Brynjólfsson[c], Tzyy Haur Chong[d,e], Bing Wu[a,*]

[a] Faculty of Civil and Environmental Engineering, University of Iceland, Hjardarhagi 2-6, IS-107, Reykjavik, Iceland
[b] HSR Hochschule für Technik Rapperswil, Institute of Environmental and Process Engineering (UMTEC), Oberseestrasse 10, 8640, Rapperswil, Switzerland
[c] Faculty of Industrial Engineering, Mechanical Engineering and Computer Science, University of Iceland, Hjardarhagi 2-6, IS-107, Reykjavik, Iceland
[d] Singapore Membrane Technology Centre, Nanyang Environment and Water Research Institute, Nanyang Technological University, 1 Cleantech Loop, 637141, Singapore
[e] School of Civil and Environmental Engineering, Nanyang Technological University, 50 Nanyang Avenue, 639798, Singapore

ARTICLE INFO

Keywords:
Algae pollution
Gravity-driven membrane filtration
LC-OCD
Membrane fouling
Surface water treatment

ABSTRACT

This study compared the membrane performances and water quality of gravity-driven membrane (GDM) systems in treating algae-polluted lake water under different operation conditions (microfiltration (MF) *vs.* ultrafiltration (UF); *Chlorella vulgaris* (green algae) *vs. Phaeodactylum tricornutum* (diatom); different algal amounts in the lake water). The results showed the cake layer fouling was predominant in the UF-GDM systems, while irreversible fouling contributed majorly to the MF-GDM fouling. As a result, the UF-GDM systems achieved > 1.5 time higher permeate flux compared to the MF-GDM systems in treating algae-polluted lake water. Compared to the green algae, the presence of the diatom cells in the feed water had more negative impacts on the UF permeate flux (increasing the cake layer resistance) and water quality (containing more low molecule weight neutrals). The analysis of cake layer foulants revealed that more aromatic protein-based biopolymers were accumulated on the membranes during filtration of algae-polluted lake water and the biopolymer amounts were almost linearly associated with membrane fouling potential of the GDM systems.

1. Introduction

Membrane-based processes (such as ultrafiltration (UF), nanofiltration (NF), reverse osmosis (RO)) has received increasing attention in treating various types of surface water for drinking water production, especially with improved membrane performance and decreased membrane cost [1]. However, membrane fouling is a major drawback in membrane-based water treatment processes. Therefore, periodically physical and chemical cleaning are required in order to achieve sustainable membrane operation, which results in consuming high energy and shortening membrane lifespan [2]. In addition, the high-frequent cleaning procedures increase the operation complexity of pressure-driven membrane processes. Such shortcomings of pressure-driven membrane processes may limit their applications in developing countries, especially for decentralized drinking water treatment in remote rural areas.

Recently, gravity-driven membrane (GDM) filtration has shown a great potential as an extremely low-energy surface water treatment process because of water gravity (40 − 100 cm) as a driving force [3]. Importantly, GDM filtration can achieve relatively stable flux without any physical and chemical cleaning during a long period of operation time. This flux stabilization phenomenon is associated with the biological behaviors of the biofilm (*i.e.* a mini-ecological system) developed on the membrane. In detail, in the biofilm layer, the prokaryotes play roles in degrading organics from the feed water and are predated by the eukaryotes, whose movement leads to form more heterogeneous and porous biofilm layer. As a consequence, the stable membrane flux is maintained [4–7]. Because of low cost and easy maintenance, the GDM systems have been successfully scaled-up and applied in treating surface water for drinking water production in remote areas of developing countries [8] and in case of disaster [9].

Nowadays, the surface water contaminations are unexpectedly occurred, which are caused by the discharges of untreated/insufficient-treated industrial, municipal, agricultural wastewaters, illegal garbage disposal, and leakage of leachate from landfills [10]. One of typical pollutants in the surface water was algae, and especially harmful cyanobacterial bloom has been paid great attention due to their production of toxic microcystins (harmful to living creatures). For example, previous studies focusing on GDM systems in treating cyanobacteria-bloom (*Microcystis aeruginosa*) lake water found that the biofilms on the

* Corresponding author.
E-mail address: wubing@hi.is (B. Wu).
[1] The authors equally contributed to this work.

https://doi.org/10.1016/j.jwpe.2020.101257
Received 25 January 2020; Received in revised form 18 March 2020; Accepted 20 March 2020

Table 1
A summary of operation conditions of the GDM systems.

	Feed water	Algal dosage (final OD_{750} in the feed water)	Membrane	Abbreviation
Stage I	Lake water	0	MF	MF(Control)
			UF	UF(Control)
	Lake water + Green algae	0.0024	MF	MF + GA(L)
			UF	UF + GA(L)
	Lake water + Diatom	0.0024	MF	MF + DI(L)
			UF	UF + DI(L)
Stage II	Lake water	0	UF	Control
	Lake water + Green algae	0.0048	UF	GA(M)
	Lake water + Green algae	0.0096	UF	GA(H)
	Lake water + Diatom	0.0048	UF	DI(M)
	Lake water + Diatom	0.0096	UF	DI(H)

membranes could successfully reduce the amount of microcystins in the permeate water (< critical threshold concentration of 1 mg/L). This was attributed to well development of the microcystin degrading bacteria in the biofilm assemblages. Nevertheless, such algal cells could decrease the permeate flux of the GDM systems [11,12].

However, effects of non-harmful algae in the surface water on the GDM membrane performance and their membrane fouling mechanisms have not been well explored. The WHO also pointed that blooms of other algae in surface water may causing coloration, turbidity, and taste change of water after filtration because of their producing other chemicals [13]. Although the gravity-driven membranes (microfiltration (MF) or UF) are capable to highly reject most of algal cells in the surface waters due to their special nature (fine pore size, surface property), the effects of these algal metabolic products on the GDM water quality also need to be illustrated.

This study aims to study the effects of algal species and amounts in the surface water on the performances of the different GDM systems (MF and UF membranes). Two non-harmful algal species, *Chlorella vulgaris* (green algae) and *Phaeodactylum tricornutum* (diatom) were used as model algae, which represents the algae in fresh surface water and brackish surface water (*e.g.* seawater infusion into the fresh water source near coastal areas), respectively. The membrane performance, water quality, and membrane fouling mechanisms of the GDM systems were examined.

2. Materials and methods

2.1. Algal culture

Axenic *P. tricornutum* (diatom) and *C. vulgaris* (green algae) were grown with f/2 + Si and Bold's Basal medium, respectively. Their cultivations were conducted using FMT50 photobioreactors (Photon Systems Instruments, Czech Republic) with constant illumination by 630 nm Red LED (100 μmol/m^2 s), controlled at a temperature of 22°C and aeration of 1 L air/L medium/min according to methods described in the previous studies [14,15]. When the algal growth reached to the stationary phase, the algal solution was collected for use. The optical density (OD) of the algal solution was measured by a spectrometer (Hach, US) at a wavelength of 750 nm (*i.e.* OD_{750}). The morphologies of the algal cells were observed by a microscopy (Nikon, Japan), shown in Fig. S1. It is noted that the *C. vulgaris* cells were not aggregated in the culture solution, which was dissimilar to those in reactor culturing conditions [16]; while *P. tricornutum* tended to aggregate in the culture solution to form relatively large flocs.

2.2. GDM filtration system setup and operation

A schematic diagram of the GDM setup was described in Fig. S2. In each GDM setup, the feed water was added to a storage tank periodically, and pumped to a feed tank. The constant water level in the feed tank was controlled by an overflow line, which was connected to the storage tank. The overflow rate was minimized by regulating the feed pump flow rate in terms of the permeate flow rate. The membrane filtration cell was connected to the feed tank, and the distance between its permeate outlet and the feed tank water level was 75 cm (*i.e.* hydrostatic pressure of 75 mbar). The permeate of membrane filtration cell was collected in a plastic bottle and weighed using an electric scale (OHAUS, USA) daily.

The membrane filtration cell was made of transparent acrylic and the top had a glass window which allowed observation of the biofouling layer morphology. A flat sheet polysulfone UF membrane (100 kDa, Microdyn Nadir, Germany) or a flat sheet hydrophilized polyvinylidene fluoride (PVDF) MF membrane (0.1 μm, Synder Filtration, US) with a membrane area of 20.7 cm^2 was placed in the filtration cell. The clean membranes were soaked in distilled water for 24 h to remove impurities before use.

The feed surface water was collected from a lake (Vatnsmýrin Nature Reserve) near University of Iceland weekly and stored at the lab for use. The algae-polluted lake water was prepared by dosing certain volume of the algal culture solution (OD_{750} at ~0.5) into the lake water. In the lab, the temperature was kept at 20 ± 1 °C and the light-dark cycle was almost at 8 h–16 h (nature light condition, *i.e.* the light intensity may change due to weather condition).

Table 1 summarizes the operation conditions of the GDM systems in this study. In the stage I, six GDM systems were operated in parallel for 10 days in order to illustrate the effects of membrane types and algal species on the GDM performance. In the following stage II, five GDM systems were operated in parallel for 34 days in order to examine the effect of algal amount in the lake water on the UF-GDM performance.

2.3. Fouling resistance analysis

The intrinsic membrane resistance (R_m), cake layer resistance fouling resistance (R_c), irreversible fouling resistance (R_{ir}), and irremovable fouling resistance (R_{im}) were evaluated using resistance-in-series model based on Darcy's Law, which was described in our previous studies [17,18]. In detail, at the end of a filtration experiment, the total hydraulic resistance ($R_t = R_m + R_c + R_{ir} + R_{im}$) was calculated based on $R_t = TMP/(\mu J)$, in which μ is the permeate viscosity, J is the measured permeate flux, and TMP is the transmembrane pressure (75 mbar). After that, the membrane was physically washed using distilled water (5 min) to remove cake layer foulants. The flux of the physically-cleaned membrane was examined using distilled water at the hydrostatic pressure of 75 mbar and the resistance ($R_m + R_{ir} + R_{im}$) was calculated. Then, the physical-cleaned membrane was soaked at 0.25 % of NaClO solution for 2 h. The flux of the chemically-cleaned membrane was examined using distilled water at the hydrostatic pressure of 75 mbar and the resistance ($R_m + R_{im}$) was calculated. The intrinsic membrane resistance (R_m) was measured using distilled water before use. The cake layer fouling resistance (R_c) was derived from the difference between R_t and ($R_m + R_{ir} + R_{im}$); The irreversible fouling resistance (R_{ir}) was achieved based on the difference between

($R_m + R_{ir} + R_{im}$) and ($R_m + R_{im}$); The irremovable fouling resistance (R_{im}) was achieved based on the difference between ($R_m + R_{im}$) and R_m.

2.4. Water quality analysis

The turbidity, pH, dissolved oxygen (DO), and conductivity measurements were conducted with a turbidity meter (Hach, US), a pH meter (Hach, US), a DO meter (Hach, US), and a conductivity meter (Hach, US), respectively. The water samples were periodically taken from the GDM systems operated at the Stage II for water quality examination. The dissolved total organic carbon (TOC) and total nitrogen in the water samples were measured by a TOC/TN analyzer (Shimadzu, Japan) after the samples was filtered with a syringe membrane (0.45 μm, Millipore, USA).

Soluble organic fractions in the water sample were measured by an LC-OCD analyzer (DOC-LABOR, Germany), which consists of a size-exclusion chromatography, an organic carbon detector, and an organic nitrogen detector. The organic matters were identified into five different fraction groups according to their molecular weights (MW), namely, biopolymers (MW > 20 kDa), humic substances (MW ~1000 Da), building blocks (MW ~300 − 500 Da), low molecular weight (LMW) acids and neutrals (MW < 350 Da). The detailed LC-OCD operation and analysis methods were described in the literature [19].

In addition, the composition of soluble organic fractions in the water sample was further identified by an EEM fluorescence spectrophotometer (Agilent, USA) at the excitation wavelength of 220 − 450 nm and the emission wavelength of 280 − 550 nm. The aromatic proteins (Region I: Ex < 250 nm, Em < 330 nm and Region II: Ex < 250 nm, Em < 380 nm), fulvic acid-like matters (Region III: Ex < 250 nm, Em > 380 nm), soluble microbial byproduct-like matters (Region IV: Ex = 250 − 280 nm, Em < 380 nm), and humic acid-like matters (Region V: Ex > 250 nm, Em > 380 nm) were identified [20].

To illustrate statistical significance, a two-sample *T*-test was performed by comparing the sampling data groups under two different conditions. The *p*-value for the two-sample *T*-test was calculated at a significance level at 5 %.

2.5. Biofilm analysis

At the end of the GDM filtration, the membrane was taken from the filtration cell. The biofilm cake layer was physically removed from the membrane by rinsing with 10 mL of distilled water (10 min), which was considered as biofilm solution. The soluble components in the biofilm solution were separated from the pellets by centrifuging at 4000 rpm for 10 min. The soluble organic compositions in the biofilm were further analyzed as the methods described in Section 2.4. The pellet foulants were collected and dried for weight measurement [21]. The specific cake resistance (m/kg) was calculated by dividing the cake layer resistance (m^{-1}) to the cake layer foulant mass load on the membrane (kg/m^2).

3. Results and discussion

3.1. Effect of membrane type and algal species on GDM performance

In this study, *Chlorella vulgaris* (unicellular eukaryotic green algae with a spherical shape at sizes of 2 − 10 μm in diameter) and *Phaeodactylum tricornutum* (fusiform shape; a very widely studied marine diatom) were selected as model pollutant algae in fresh surface water and in brackish surface water, respectively.

Shown in Fig. 1, during 10-day's GDM filtration (Stage I), the permeate fluxes dramatically dropped during initial period of filtration (within the first day) before they stabilized, regardless of membrane type and algal species. This phenomenon has well been observed in the GDM systems in treating different types of water (surface water [6], seawater [22], rainwater [23], grey water [24], wastewater [17]). It was thought the initial membrane fouling was mainly induced by pore constriction in the GDM systems, significantly limiting water passing through the membranes and subsequently leading to a sudden drop of the permeate flux [25].

After 10-day operation, the averaged permeate flux remained considerably stable at ~2.54, ~1.45, ~2.03 L/m^2h in the MF-GDM systems treating the lake water, green algae-polluted lake water and diatom-polluted lake water, respectively, which were relatively lower than those in the UF-GDM systems (~6.55, ~9.42, ~5.53 L/m^2h for the lake water, green algae-polluted lake water and diatom-polluted lake water, respectively; Table S1). Obviously, the presence of both types of algae in the lake water led to an obvious decrease of the MF-GDM permeate fluxes. In the UF-GDM systems, the permeate flux was slightly improved when a low amount of green algae was dosed in the lake water, while a low amount of diatom in the lake water caused a slightly reduced permeate flux of the UF-GDM system.

Furthermore, the fouled membrane morphologies were recorded (Fig. S3) and the fouling resistance distribution was evaluated (Fig. 2). In the MF-GDM systems treating the lake water (*i.e.* MF(control)), the irreversible fouling was predominant, contributing to 52 % of total fouling resistance. When the lake water was dosed with algae, both irreversible fouling resistance ($1.2–1.3 \times 10^{13}\ m^{-1}$) and irremovable fouling resistance ($1.9–2.2 \times 10^{12}\ m^{-1}$) greatly increased in the MF-GDM systems, while their cake layer fouling resistances were much lower than that in the MF(control). In contrast, the cake layer fouling contributed majorly to the total fouling in the UF-GDM systems in the absence and presence of additional algal species, ranging from 87 to 93 %. Compared to the control UF-GDM system ($3.6 \times 10^{12}\ m^{-1}$), the dosed green algae in the UF-GDM system led to a slight decrease of cake layer fouling resistance ($2.6 \times 10^{12}\ m^{-1}$), while the dosed diatom caused an increase of cake layer fouling ($4.7 \times 10^{12}\ m^{-1}$).

Such observations suggest that the UF-GDM systems had better membrane performance and experienced less negative effects by the low amount of dosed algae in the lake water compared to the MF-GDM systems. It is noticed that the pristine UF membrane (averaged at ~90 L/m^2h) had a higher clean water flux than the MF membrane (averaged at ~27 L/m^2h) at a hydrostatic pressure of 75 mbar. While, the clean membrane resistances only contributed < 10 % of the total fouling resistance for both types of membranes (Fig. 2). Thus, such difference in the clean membrane permeability may not be the major reason for the better performance of the UF membrane. Indeed, the different fouling mechanisms of the MF and UF membranes appeared to be associated with their performances. As shown in Figs. 2 and S3, most of the potential foulants in the lake water could be rejected by the UF membrane to form a cake layer, while these foulants appeared to predominantly plug or narrow the pores of the MF membrane possibly due to their relatively comparable sizes to the MF membrane pore sizes. Furthermore, the rejected organics on the UF membrane surface could benefit the prokaryotes development, as a result, promoting the eukaryotic predation and movement activity. Accordingly, more heterogeneous and porous biofilm layer was formed on the UF membrane (although more biofilm mass), which resulted in a higher permeate flux [4,5,22]. Additionally, the lower amount of algal cells (especially green algae) may behave as dosed particles, which could facilitate the formed cake layer with much more heterogeneous nature, as a result, leading to less cake layer filtration resistance [26,27].

It is also observed that the influences of algal species on the performances of the MF-GDM and UF-GDM systems behaved in different patterns. In the MF-GDM system fed with green algae-dosed lake water, a lower permeate flux was observed due to more cake layer, irreversible, and irremovable fouling resistances compared to those with diatom-dosed lake water. While, the presence of the green algae in the lake water benefited to increase the permeate flux in the UF-GDM systems by reducing reversible fouling.

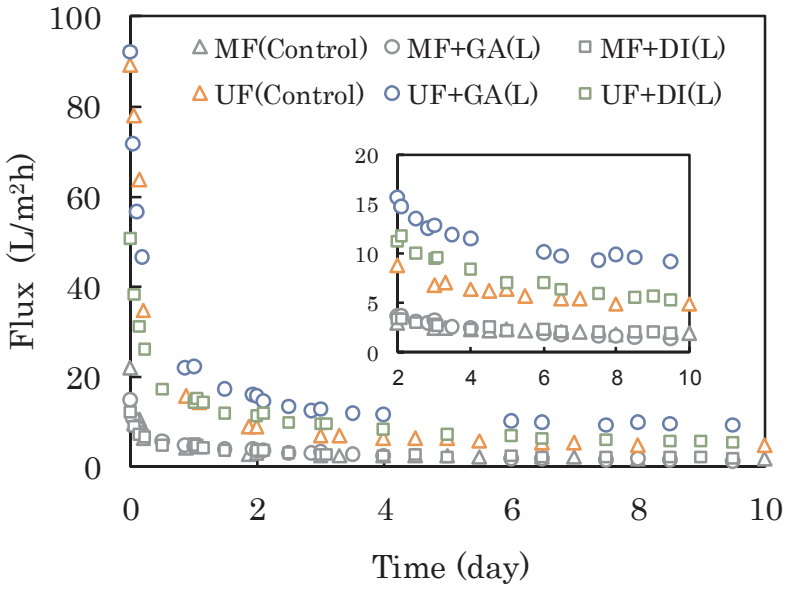

Fig. 1. Flux developments of GDM systems with different membranes and algal species.

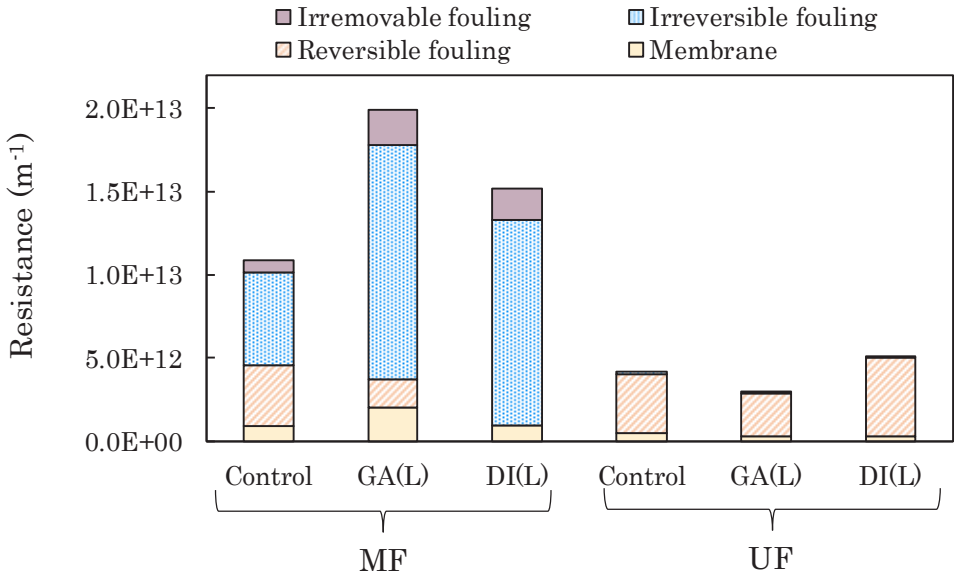

Fig. 2. Membrane fouling resistance distribution in GDM systems with different membranes and algal species.

3.2. Effect of algal concentration on GDM performance

3.2.1. Membrane performance and fouling resistance distribution

As the UF-GDM systems had better membrane performance than the MF-GDM systems and a lower amount of algae in the lake water had insignificant impacts on the UF-GDM performance (Stage I), in the stage II, the effect of higher algal concentration (2-time and 4-time of the algal concentration in the stage I) on the UF-GDM performance was further explored. The GDM permeate flux development profiles were presented in Fig. 3.

Similarly, the permeate fluxes dramatically dropped during initial period of filtration (within the first day) before they stabilized under all testing conditions (Fig. 3). Compared to the stable flux in the control GDM (~9.00 L/m^{2}h), the presence of more algal cells in the lake water could lead to decreased permeate fluxes for both algal species (~2.97 – 7.23 L/m^{2}h). It is noted that the control UF-GDM systems in the stage I and II had slightly different stable fluxes (~6.22 and ~9.00 L/m^{2}h respectively; Table S1) because the feed lake water taken at different periods of time had slightly dissimilar compositions (*e.g.* turbidity, 23.3 ± 8.8 NTU *vs.* 6.2 ± 7.6 NTU, Tables S2 and 2). To make a fair comparison, the flux incline or decline ratio was calculated and illustrated in Table S1. Obviously, when a lower concentration of green algae was present in the lake water, the permeate flux increased 44 %, while with further increasing its concentration to 2× and 4×, the permeate flux dropped 20 % and 23 %, respectively. In the presence of the diatom in the lake water, the permeate flux decreased from 16 % to 34 %, to 67 % with elevating the diatom concentration from 1× to 2×, to 4×, respectively.

At the end of experiments (Day 34), the fouling resistance distribution was further examined, shown in Fig. 4. The cake layer fouling was predominant in the higher amount of algae-dosed GDM systems at the Stage II, similar to the control GDM system and the GDM system with the lower amount of algae (UF membrane, Stage I). It was also observed that the permeate flux decline was associated with an increased cake layer fouling. Moreover, the amounts of the diatom cells in the feed lake water had a more significant impact on the GDM

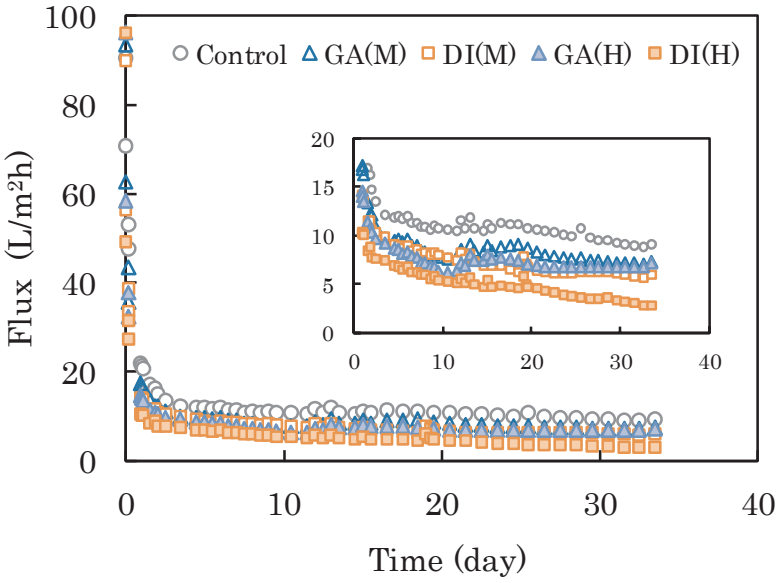

Fig. 3. Flux development profiles of UF-GDM systems treating feed water with different algal concentrations.

performance than those of the green algae.

3.2.2. Permeate water quality

The water samples from the feed water tanks and permeate bottles were periodically monitored during 34-day operation (Stage II) and their water quality parameters were presented in the Table 2. As shown in Table 2, dosing both algal cells into the feed water could not significantly influence turbidity, pH, and DO levels compared to the control feed (*i.e.* without dosing algae; *p*-values > 0.05). In contrast, dosing the diatom cell solution (including cultural medium) could significantly increase the feed water conductivity (*p*-value < 0.05) because the dosed cultural medium was at a high salinity level, while the conductivity of the feed water dosed with the green algae was not significantly varied (*p*-value > 0.05). The permeate water in all tested GDM systems was almost turbidity-free due to excellent rejection of the UF membranes. In addition, the pH, DO, or conductivity level in the permeate water was comparable to that in its respective feed water.

In addition, compared to the control feed water, the diatom-dosed feed water had greatly more soluble organic carbon and total nitrogen (*p*-value < 0.05), while the feed water dosed with the green algae had similar amounts of soluble organic carbon and total nitrogen (*p*-value > 0.05; Table 2). As the diatom culture medium (f/2 + Si) contains Na_2EDTA ($C_{10}H_{14}N_2Na_2O_8$) trace element (~1.48 mgC/L in the culture medium), it could contribute soluble organic carbon in the diatom-dosed feed water (contributing ~15 − 30 μgC/L in the feed water as 50–100 times dilution of the culture medium). In addition, it has been reported that marine diatoms can secrete large amounts of extracellular polymeric substances (EPS) and their quantity and quality are environmental-dependent [28,29]. After the marine diatom cells were dosed into the lake water, their growth conditions shifted from favorable high salinity to unfavorable low salinity, as a result, they may regulate their metabolic behaviors by producing more EPS to tolerate such environmental stress. Especially, these led to great amount of LMW neutral substances in the diatom-dosed feed water, almost 50–100 times higher than those in the control feed water.

Furthermore, the averaged soluble TOC (15.7–18.9 %) and TN

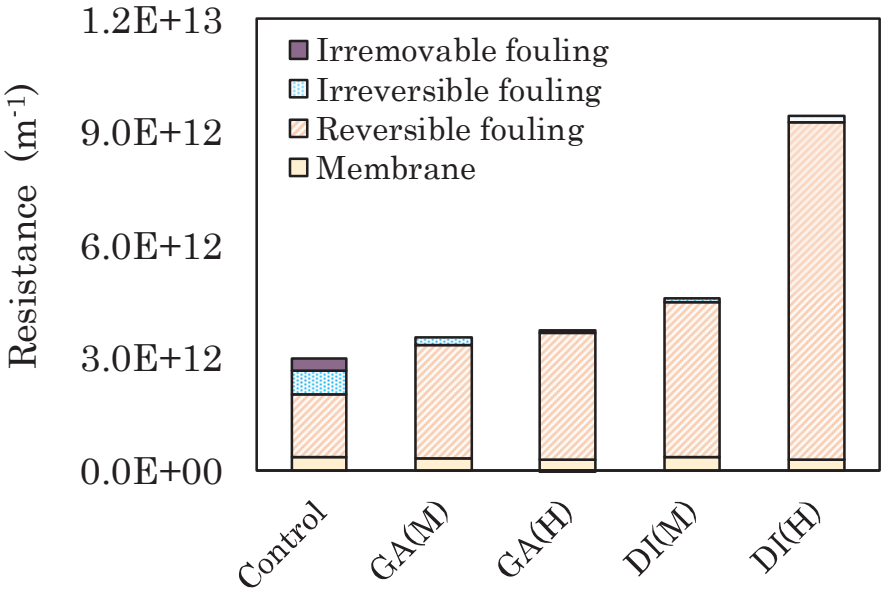

Fig. 4. Membrane fouling resistances of GDM systems (UF membrane) treating feed water with different algal concentrations.

Table 2
Water quality parameters of GDM systems in treating lake water with different algal concentrations (n > 4).

Parameter	Feed water				
	Control	GA(M)	GA(H)	DI(M)	DI(H)
Turbidity (NTU)	6.2 ± 7.6	3.5 ± 3.3	2.2 ± 1.3	2.5 ± 1.7	2.6 ± 1.9
DO (mg/L)	8.6 ± 0.2	7.7 ± 0.5	7.5 ± 0.5	8.8 ± 0.3	8.5 ± 0.3
pH	8.5 ± 0.1	8.2 ± 0.1	8.2 ± 0.2	8.4 ± 0.1	8.3 ± 0.1
Conductivity (μS/cm)	647 ± 72	609 ± 65	611 ± 62	1821 ± 227	3052 ± 338
Soluble TOC (mg/L)	5.09 ± 2.56	5.48 ± 2.41	5.47 ± 2.01	20.02 ± 6.14	39.18 ± 7.25
Soluble TN (mg/L)	1.00 ± 0.19	0.58 ± 0.43	0.93 ± 0.41	6.44 ± 0.90	12.19 ± 1.25
Biopolymers (μg/L)	72 ± 44	156 ± 88	96 ± 49	175 ± 146	113 ± 37
Humic substances (μg /L)	974 ± 82	1009 ± 221	1099 ± 170	1005 ± 269	1191 ± 63
Building blocks (μg /L)	254 ± 50	429 ± 131	462 ± 150	306 ± 133	422 ± 103
LMW neutrals (μg /L)	316 ± 132	410 ± 123	369 ± 95	15989 ± 2557	33067 ± 5901
LMW acids (μg /L)	ND	ND	ND	ND	ND
Parameter	Permeate water				
	Control	GA(M)	GA(H)	DI(M)	DI(H)
Turbidity (NTU)	ND	ND	ND	ND	ND
DO (mg/L)	8.8 ± 0.3	8.8 ± 0.2	8.8 ± 0.2	8.8 ± 0.2	8.7 ± 0.2
pH	8.5 ± 0.1	8.4 ± 0.0	8.4 ± 0.1	8.3 ± 0.0	8.3 ± 0.0
Conductivity (μS/cm)	659 ± 75	565 ± 35	547 ± 32	2012 ± 398	3150 ± 342
Soluble TOC (mg/L)	4.42 ± 1.75	4.24 ± 1.50	4.43 ± 1.27	20.31 ± 3.48	36.06 ± 5.98
Averaged TOC removal (%)	~12.5	~18.9	~15.7	~3.8	~7.6
Soluble TN (mg/L)	0.9 ± 0.15	0.55 ± 0.17	1.01 ± 0.11	6.12 ± 0.81	11.64 ± 0.63
Averaged TN removal (%)	~2.4	~7.7	~11.6	~3.0	~2.0
Biopolymers (μg /L)	98 ± 64	138 ± 57	98 ± 15	148 ± 106	65 ± 2
Humic substances (μg /L)	1088 ± 254	1165 ± 318	1136 ± 348	1020 ± 116	1111 ± 203
Building blocks (μg /L)	299 ± 76	354 ± 144	458 ± 107	435 ± 106	474 ± 97
LMW neutrals (μg /L)	376 ± 151	312 ± 100	351 ± 111	16309 ± 1887	30846 ± 4696
LMW acids (μg /L)	45 ± 87	2 ± 4	ND	ND	24 ± 47

(7.7–11.6 %) removal ratios of the green algae-dosed GDM systems were slightly higher than those in the control GDM (12.5 % and 2.4 %, respectively). Both removal ratios were improved with increasing dosing amount of the green algae. Previous studies have pointed out that the green algae *C. vulgaris* could utilize organic carbon sources to promote their growth (*i.e.* heterotrophic and mixotrophic growth) [14,30] and enhance nutrient removal from the wastewater [31]. This characteristics of green algae promoted the organic removal efficiencies in the GDM systems. While, in the diatom-dosed GDM systems, the averaged soluble TOC removal ratios (3.8–7.6 %) were lower than that in the control GDM (12.5 %) and TN removal ratios (2–3 %) were comparable to that in the control GDM (2.4 %).

To further investigate the effect of algal species and concentrations on DOC removal, compositions of DOC were analyzed by LC-OCD (Table 2) and EEM (Fig. 5). Table 2 shows that in both control GDM and algae-dosed GDM systems, the concentrations of all five organic components in the permeate were slightly higher than or comparable to those in respective feed water. Similarly, the EEM analysis results (Fig. 5) also indicated that almost comparable amounts of five types of organic components in the feed and permeate water. This phenomenon was also observed in the previous studies [17,18,32–34]. It was speculated that (1) the particulate organics (not measured by the TOC analyzer due to pretreatment procedure of TOC analysis) in the feed water could decomposed or hydrolyzed into the smaller-sized soluble substances, and (2) the microorganisms on the membrane surface utilized greater-sized organics and produced smaller-sized soluble substances. These soluble substances could not be effectively retained by the UF membranes and therefore were present in the permeate.

3.2.3. Cake layer foulants characteristics

The cake layer morphologies were directly observed *via* the glass windows of the GDM filtration cells and their photos were recorded in Fig. S4. Clearly, the algal cells covered the membrane surface within the first day of filtration, showing being highly retained by the membranes. With more particulates from the lake water accumulated on the membranes, the algal presence (especially green algae) was not obviously noticed. At the end of filtration experiments, the cake layer was carefully removed from the membrane surface and the foulant characteristics were examined. The microscopic images in the Fig. S5 revealed the presence of the eukaryotes in the cake layer, regardless of the absence and presence of dosed algal cells.

Shown in Table 3, much more cake layer foulants were deposited on the membrane surface in the GDM systems treating algae-dosed lake water compared to those in the control GDM system. This was attributed to the accumulation of the rejected algal cells on the UF membranes (Fig. S3). In terms of the accumulated foulant mass load on the membrane, the specific cake resistance was calculated and presented in Table 3. Apparently, the specific cake resistances in the GMD systems treating the green algae-dosed lake water and the diatom-dosed lake water were almost > 7.8-time and > 3.4-time lower than that fed with the control lake water, respectively. This implies that in the presence of algal cells (especially the green algae) in the lake water, the formed cake layer on the UF membrane would be more porous compared to that in the control condition.

Furthermore, the accumulated organic substances on the membrane surfaces were examined, presented in Table 4. With increasing dosing algal cells in the feed water, more soluble organics (in term of soluble TOC) were deposited on the membrane surface. This implies that the amounts of soluble organics in the cake layers were associated with the GDM permeate flux (Fig. 1). This observation was dissimilar with the finding in a previous study [35] that the accumulated TOC amounts did not significantly influence the permeate flux of GDM systems in treating secondary wastewater effluent treatment. Such difference was possibly associated with different wastewater characteristics (lake water *vs.* secondary wastewater effluent) and membrane properties (100 kDa *vs.* 20 kDa) in these two studies.

In addition, the fractions of soluble organic substances in the biofilm cake layer were examined by LC-OCD and EEM (Table 4). The LC-OCD results indicated that the biopolymers were the major organic foulants in the GDM systems (52–71 %), regardless of absence or presence of the

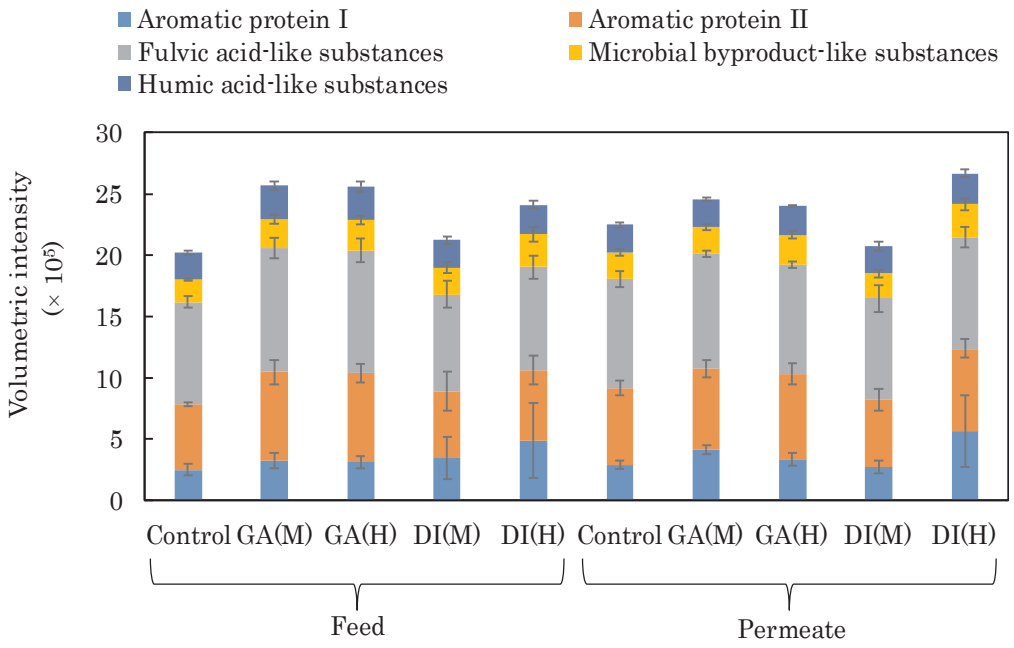

Fig. 5. EEM analysis of soluble organics in the feed and permeate water.

Table 3
The characteristics of foulants derived from GDM systems in treating lake water with different algal concentrations.

	Control	GA(M)	GA(H)	DI(M)	DI(H)
Mass load (kg/m^2)	0.0025	0.0433	0.0436	0.0206	0.0634
Specific cake resistance (m/kg)	6.8E+14	7.0E+13	7.7E+13	2.0E+14	1.4E+14

algal cells in the feed water. The amounts of biopolymers on the membranes in the GDM systems treating the diatom-dosed lake water (23.1–46.4 mg/m^2) were remarkably higher than those with the green algae-dosed feed water (20.7–26.9 mg/m^2), both of which were greater than that in the control reactor (9.2 mg/m^2). It is well documented that both *Chlorella vulgaris* (green algae) and *Phaeodactylum tricornutum* (diatom) have capability in producing valuable organic components (such as lipids, proteins) [28,36]. Possibly, the deposited algal cells on the membrane surface could produce such greater-sized organics (*i.e.* biopolymers), which were retained by the UF membranes.

Increasing the amount of the diatom cells in the feed water could promote the biopolymer accumulation on the membrane, while an insignificant increase of biopolymer deposition amounts on the membranes was noticed with increasing green algae concentration in the feed water. Nevertheless, the amount of biopolymers was highly correlated with the cake layer resistance ($R^2 = 0.91$), instead of the amounts of other organic fractions (*i.e.* humic substances, building blocks and LMWs). A similar finding was also reported in the GDM systems in treating municipal wastewater [17].

The EEM analysis further revealed that in all tested five GDM systems, the fluorescence intensities of aromatic proteins (I and II) were greater than those of fulvic-like substances (III), microbial byproduct-like substances (IV), and humic-like substances (V), accounting to 55–68 % of the total five organic components. In addition, the presence of green algae in the GDM systems appeared to promote more aromatic protein accumulation on the membranes compared to the control and diatom-dosed GDM systems. This trend is not consistent with the findings in LC-OCD. Possibly, certain organics (especially biopolymers) that could be detected by LC-OCD may not have florescent characteristics, as a result, they were not presented in EEM fractions.

Nevertheless, the algal species in the polluted water could influence GDM performance due to their dissimilar membrane fouling mechanisms (in terms of foulant characteristics), which were associated to their respective physiological behaviors under GDM operation conditions. Previous study also highlighted that the exposed light intensity could influence GDM performance due to its effect on algal growth [37]. Due to greatly dissimilar light condition during Summer and Winter in

Table 4
The characteristics of soluble foulants derived from GDM systems in treating lake water with different algal concentrations.

Soluble foulants		Control	GA (M)	GA (H)	DI (M)	DI (H)
LC-OCD analysis (mg/m^2)	Soluble TOC (mg/m^2)	50.6	129.9	137.8	114.6	179.4
	Soluble TN (mg/m^2)	8.0	24.5	22.2	33.7	46.7
	Biopolymers	9.2	20.7	26.9	23.1	46.4
	Humic substances	1.9	0.0	0.0	0.0	0.0
	Building blocks	2.2	6.7	9.1	11.0	12.7
	LMW neutrals	4.3	6.6	5.4	5.8	6.3
	LMW acids	0.0	0.3	0.4	0.4	0.4
EEM analysis (×10^6 intensity /m^2)	Aromatic protein I	2.9	4.4	4.8	2.7	2.8
	Aromatic protein II	3.8	5.4	6.0	3.8	3.2
	Fulvic acid-like substances	1.7	2.5	2.0	2.2	1.4
	Microbial byproduct-like substances	1.6	2.6	2.7	2.3	2.0
	Humic acid-like substances	0.5	0.8	0.5	0.7	0.6

Iceland, future study on the effect of seasonal condition on GDM performance in treating algae-contained surface water was proposed.

4. Conclusions

The effects of membrane types, algae species and concentrations on the performances of the GDM systems were investigated in terms of permeate flux, water quality, and membrane fouling mechanisms and characterization. The results showed the presence of algal cells in the feed water could dramatically increase irreversible fouling of MF membranes, while it caused an insignificant increase of cake layer fouling of UF membranes, especially at lower algal concentrations. In addition, increasing the concentrations of algal cells in the feed water could cause more cake layer fouling due to the accumulation of more biopolymers on the UF membranes. Meanwhile, greater amount of LMW neutrals was observed in the permeate water of the GDM systems treating diatom-polluted lake water, while the green algae in the feed water did not significantly influence the permeate quality of GDM systems.

Declaration of Competing Interest

The authors declare that they have no known competing financial interests or personal relationships that could have appeared to influence the work reported in this paper.

Acknowledgements

This study was supported by the University of Iceland Research Fund. The authors appreciate Prof. Snædís Huld Björnsdóttir for providing microscopy facility and Prof. Sigurður Erlingsson for providing lab space.

Appendix A. Supplementary data

Supplementary material related to this article can be found, in the online version, at doi:https://doi.org/10.1016/j.jwpe.2020.101257.

References

[1] J. Hoslett, T.M. Massara, S. Malamis, D. Ahmad, I. van den Boogaert, E. Katsou, B. Ahmad, H. Ghazal, S. Simons, L. Wrobel, H. Jouhara, Surface water filtration using granular media and membranes: a review, Sci. Total Environ. 639 (2018) 1268–1282.
[2] H.Q. Chang, H. Liang, F.S. Qu, B.C. Liu, H.R. Yu, X. Du, G.B. Li, S.A. Snyder, Hydraulic backwashing for low-pressure membranes in drinking water treatment: a review, J. Membr. Sci. 540 (2017) 362–380.
[3] W. Pronk, A. Ding, E. Morgenroth, N. Derlon, P. Desmond, M. Burkhardt, B. Wu, A.G. Fane, Gravity-driven membrane filtration for water and wastewater treatment: a review, Water Res. 149 (2019) 553–565.
[4] N. Derlon, N. Koch, B. Eugster, T. Posch, J. Pernthaler, W. Pronk, E. Morgenroth, Activity of metazoa governs biofilm structure formation and enhances permeate flux during Gravity-Driven Membrane (GDM) filtration, Water Res. 47 (6) (2013) 2085–2095.
[5] N. Derlon, M. Peter-Varbanets, A. Scheidegger, W. Pronk, E. Morgenroth, Predation influences the structure of biofilm developed on ultrafiltration membranes, Water Res. 46 (10) (2012) 3323–3333.
[6] M. Peter-Varbanets, F. Hammes, M. Vital, W. Pronk, Stabilization of flux during dead-end ultra-low pressure ultrafiltration, Water Res. 44 (12) (2010) 3607–3616.
[7] M. Peter-Varbanets, J. Margot, J. Traber, W. Pronk, Mechanisms of membrane fouling during ultra-low pressure ultrafiltration, J. Membr. Sci. 377 (1-2) (2011) 42–53.
[8] M. Boulestreau, E. Hoa, M. Peter-Verbanets, W. Pronk, R. Rajagopaul, B. Lesjean, Operation of gravity-driven ultrafiltration prototype for decentralised water supply, Desalin. Water Treat. 42 (1–3) (2012) 125–130.
[9] F.B. Frechen, H. Exler, J. Romaker, W. Schier, Long-term behaviour of a gravity-driven dead end membrane filtration unit for potable water supply in cases of disasters, Water Sci. Technol.-Water Supply 11 (1) (2011) 39–44.
[10] H.A. Hasan, M.H. Muhammad, N.I. Ismail, A review of biological drinking water treatment technologies for contaminants removal from polluted water resources, J. Water Process Eng. 33 (2020) 101035.
[11] E. Kohler, J. Villiger, T. Posch, N. Derlon, T. Shabarova, E. Morgenroth, J. Pernthaler, J.F. Blom, Biodegradation of Microcystins during Gravity-Driven Membrane (GDM) ultrafiltration, PLoS One 9 (11) (2014).
[12] M.O.D. Silva, P. Desmond, N. Derlon, E. Morgenroth, J. Pernthaler, Source community and assembly processes affect the efficiency of microbial microcystin degradation on drinking water filtration membranes, Front. Microbiol. 10 (2019).
[13] World Health Organization, Guidelines for Drinking-Water Quality: Fourth Edition Incorporating the First Addendum, World Health Organization, Geneva, 2017 Licence: CC BY-NC-SA 3.0 IGO.
[14] W.Q. Fu, S. Gudmundsson, K. Wichuk, S. Palsson, B.O. Palsson, K. Salehi-Ashtiani, S. Brynjolfsson, Sugar-stimulated CO2 sequestration by the green microalga Chlorella vulgaris, Sci. Total Environ. 654 (2019) 275–283.
[15] Z.Q. Yi, Y.X. Su, M.N. Xu, A. Bergmann, S. Ingthorsson, O. Rolfsson, K. Salehi-Ashtiani, S. Brynjolfsson, W.Q. Fu, Chemical mutagenesis and fluorescence-based high-throughput screening for enhanced accumulation of carotenoids in a model marine diatom Phaeodactylum tricornutum, Mar. Drugs 16 (8) (2018).
[16] L. Fortunato, A.F. Lamprea, T. Leiknes, Evaluation of membrane fouling mitigation strategies in an algal membrane photobioreactor (AMPBR) treating secondary wastewater effluent, Sci. Total Environ. 708 (2020).
[17] S. Lee, M. Sutter, M. Burkhardt, B. Wu, T.H. Chong, Biocarriers facilitated gravity-driven membrane (GDM) reactor for wastewater reclamation: effect of intermittent aeration cycle, Sci. Total Environ. 694 (2019).
[18] B. Wu, T. Christen, H.S. Tan, F. Hochstrasser, S.R. Suwarno, X. Liu, T.H. Chong, M. Burkhardt, W. Pronk, A.G. Fane, Improved performance of gravity-driven membrane filtration for seawater pretreatment: implications of membrane module configuration, Water Res. 114 (2017) 59–68.
[19] S.A. Huber, A. Balz, M. Abert, W. Pronk, Characterisation of aquatic humic and non-humic matter with size-exclusion chromatography – organic carbon detection – organic nitrogen detection (LC-OCD-OND), Water Res. 45 (2) (2011) 879–885.
[20] W. Chen, P. Westerhoff, J.A. Leenheer, K. Booksh, Fluorescence excitation – emission matrix regional integration to quantify spectra for dissolved organic matter, Environ. Sci. Technol. 37 (24) (2003) 5701–5710.
[21] APHA, Standard Methods for the Examination of Water and Wastewater, 20th ed., American Public Health Association, Washington, DC, 1998.
[22] E. Akhondi, B. Wu, S.Y. Sun, B. Marxer, W.K. Lim, J. Gu, L.B. Liu, M. Burkhardt, D. McDougald, W. Pronk, A.G. Fane, Gravity-driven membrane filtration as pretreatment for seawater reverse osmosis: linking biofouling layer morphology with flux stabilization, Water Res. 70 (2015) 158–173.
[23] B. Wu, G.Q.Y. Soon, T.H. Chong, Recycling rainwater by submerged gravity-driven membrane (GDM) reactors: effect of hydraulic retention time and periodic backwash, Sci. Total Environ. 654 (2019) 10–18.
[24] A. Ding, H. Liang, G.B. Li, I. Szivak, J. Traber, W. Pronk, A low energy gravity-driven membrane bioreactor system for grey water treatment: permeability and removal performance of organics, J. Membr. Sci. 542 (2017) 408–417.
[25] B. Wu, F. Hochstrasser, E. Akhondi, N. Ambauen, L. Tschirren, M. Burkhardt, A.G. Fane, W. Pronk, Optimization of gravity-driven membrane (GDM) filtration process for seawater pretreatment, Water Res. 93 (2016) 133–140.
[26] A. Ding, J.L. Wang, D.C. Lin, X.B. Tang, X.X. Cheng, G.B. Li, N.Q. Ren, H. Liang, In situ coagulation versus pre-coagulation for gravity-driven membrane bioreactor during decentralized sewage treatment: permeability stabilization, fouling layer formation and biological activity, Water Res. 126 (2017) 197–207.
[27] X.B. Tang, W. Pronk, A. Ding, X.X. Cheng, J.L. Wang, B.H. Xie, G.B. Li, H. Liang, Coupling GAC to ultra-low-pressure filtration to modify the biofouling layer and bio-community: flux enhancement and water quality improvement, Chem. Eng. J. 333 (2018) 289–299.
[28] G. Pierre, J.M. Zhao, F. Orvain, C. Dupuy, G.L. Klein, M. Graber, T. Maugard, Seasonal dynamics of extracellular polymeric substances (EPS) in surface sediments of a diatom-dominated intertidal mudflat (Marennes-Oleron, France), J. Sea Res. 92 (2014) 26–35.
[29] G.J.C. Underwood, M. Boulcott, C.A. Raines, K. Waldron, Environmental effects on exopolymer production by marine benthic diatoms: dynamics, changes in composition, and pathways of production, J. Phycol. 40 (2) (2004) 293–304.
[30] T. Heredia-Arroyo, W. Wei, R. Ruan, B. Hu, Mixotrophic cultivation of Chlorella vulgaris and its potential application for the oil accumulation from non-sugar materials, Biomass Bioenergy 35 (5) (2011) 2245–2253.
[31] P.S. Lau, N.F.Y. Tam, Y.S. Wong, Wastewater nutrients removal by Chlorella vulgaris: optimization through acclimation, Environ. Technol. 17 (2) (1996) 183–189.
[32] A. Chomiak, J. Traber, E. Morgenroth, N. Derlon, Biofilm increases permeate quality by organic carbon degradation in low pressure ultrafiltration, Water Res. 85 (2015) 512–520.
[33] N. Derlon, J. Mimoso, T. Klein, S. Koetzsch, E. Morgenroth, Presence of biofilms on ultrafiltration membrane surfaces increases the quality of permeate produced during ultra-low pressure gravity-driven membrane filtration, Water Res. 60 (2014) 164–173.
[34] S.L. Shao, Y.J. Feng, H.R. Yu, J.Y. Li, G.B. Li, H. Liang, Presence of an adsorbent cake layer improves the performance of gravity-driven membrane (GDM) filtration system, Water Res. 108 (2017) 240–249.
[35] Y.R. Wang, L. Fortunato, S. Jeong, T. Leiknes, Gravity-driven membrane system for secondary wastewater effluent treatment: filtration performance and fouling characterization, Sep. Purif. Technol. 184 (2017) 26–33.
[36] C. Safi, B. Zebib, O. Merah, P.Y. Pontalier, C. Vaca-Garcia, Morphology, composition, production, processing and applications of Chlorella vulgaris: a review, Renew. Sustain. Energy Rev. 35 (2014) 265–278.
[37] S.L. Shao, D.T. Shi, Y.Q. Li, Y. Liu, Z.Y. Lu, Z. Fang, H. Liang, Effects of water temperature and light intensity on the performance of gravity-driven membrane system, Chemosphere 216 (2019) 324–330.

529 **Supplementary data**

530 **Table S1. A summary of the averaged permeate flux at different conditions**

Stage I (MF)			Stage I (UF)		
Control	GA(L)	DI (L)	Control	GA(L)	DI (L)
2.54	1.45	2.03	6.55	9.42 (44%↑)*	5.53 (16%↓)

Stage II (UF)				
Control	GA(M)	GA(H)	DI(M)	DI(H)
9.00	7.23 (20%↓)	6.96 (23%↓)	5.91 (34%↓)	2.97 (67%↓)

531 ***** The ratio in the bracket represents the permeate flux (defined as J) incline/decline ratio, which
532 is calculated as the absolute value of $[(J_{algae}-J_{control})\times 100/J_{control}]$%.

533

534 **Table S2. Water quality parameters of GDM systems with GDM systems with different**
535 **membrane types and algal species (Stage I)**

	Feed water			Permeate water (MF)			Permeate water (UF)		
	Control	GA (L)	DI (L)	Control	GA (L)	DI (L)	Control	GA (L)	DI (L)
Turbidity (NTU)	23.3±8.8	35.6±43.0	24.7±4.7	ND	ND	ND	ND	ND	ND
DO (mg/L)	8.9±0.3	8.8±0.2	8.5±0.2	8.8±0.2	8.8±0.2	8.9±0.1	8.9±0.2	8.8±0.2	8.9±0.1
pH	8.3±0.2	8.3±0.1	8.1±0.1	8.3±0.1	8.3±0.1	8.2±0.1	8.3±0.1	8.3±0.1	8.2±0.1
Conductivity (μS/cm)	813±167	675±69	1498±107	883±96	661±50	1485±124	880±73	666±57	1503±126

536

537

538

Green Algae
(*Chlorella vulgaris*)

Diatom
(Phaeodactylum tricornutum)

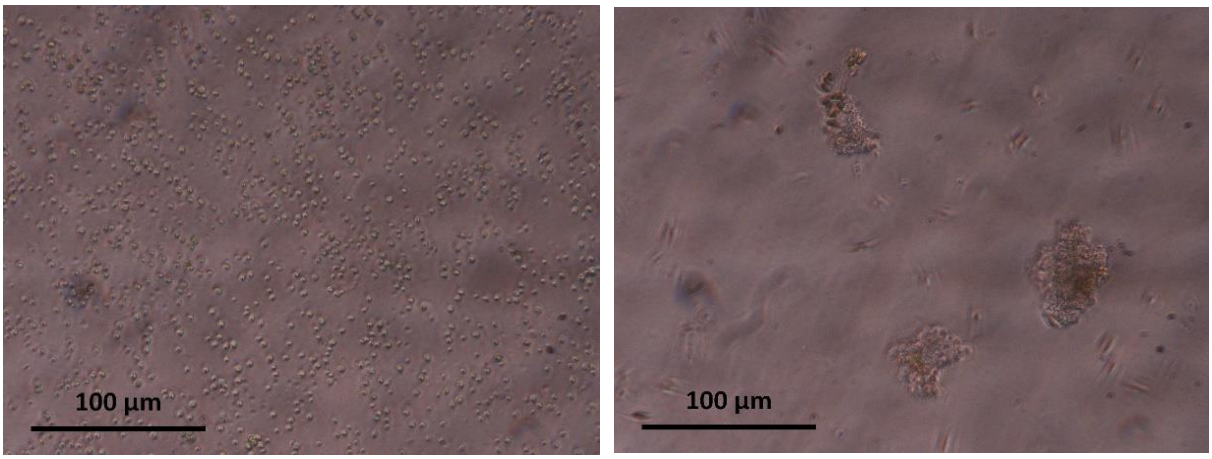

Figure S1. Microscopic images of green algae (*Chlorella vulgaris*) and diatom (*Phaeodactylum tricornutum*)

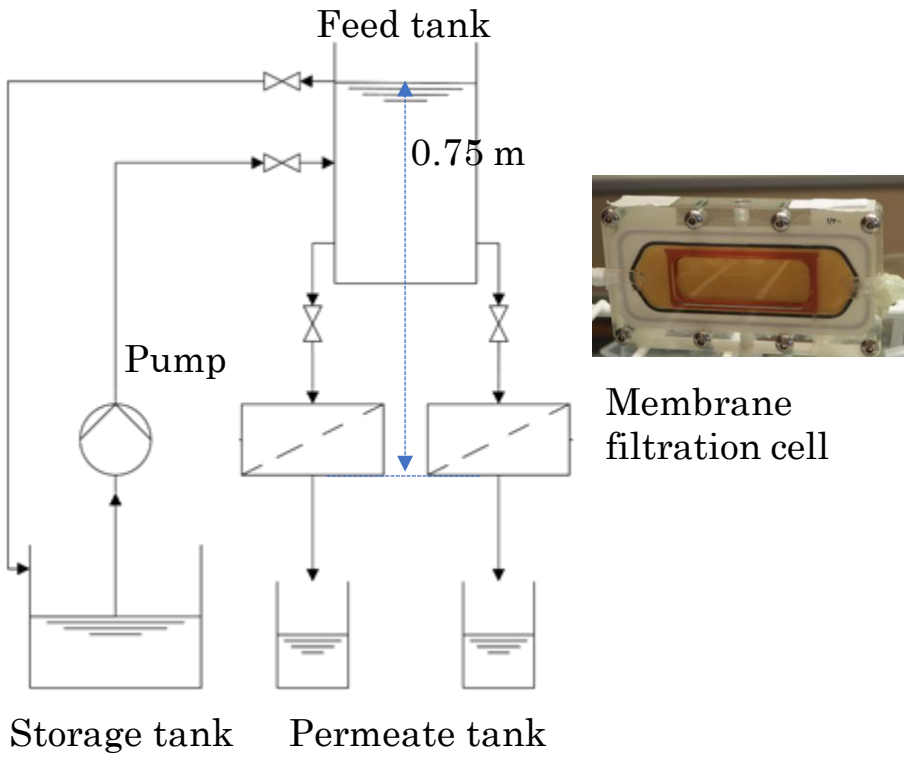

Figure S2. A schematic diagram of the GDM system. (Note: There was no any valve between the permeate out and tubing outlet, which allows the permeate water freely flowing to the collected bottle, i.e., the pressures at the permeate outlet and tubing outlet were the same as the atmosphere pressure.)

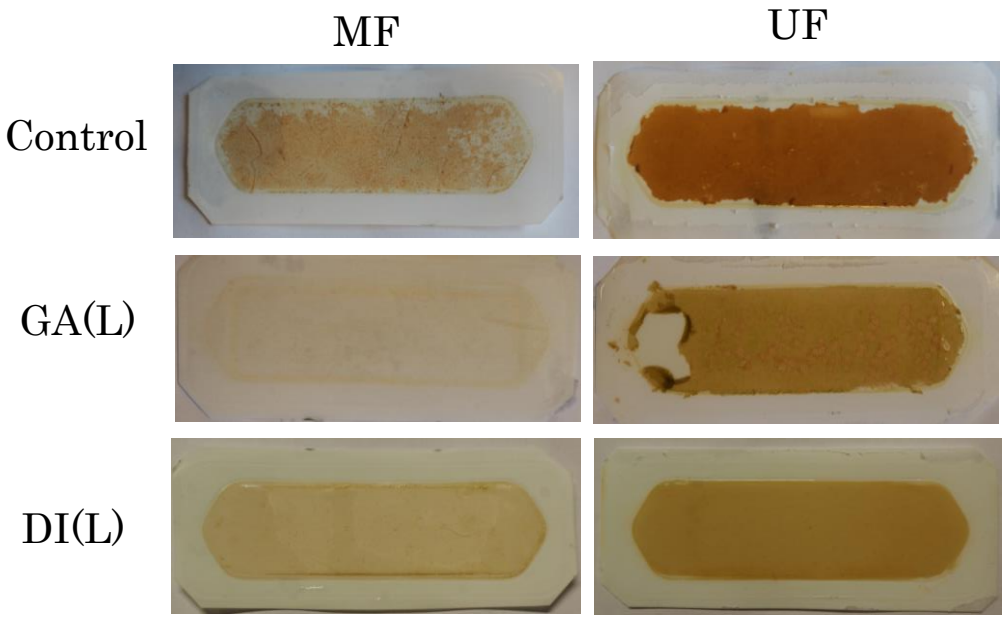

553

554 **Figure S3. Photos of the fouled membranes in the Stage I (Day 10)**

555

556

557

558

559

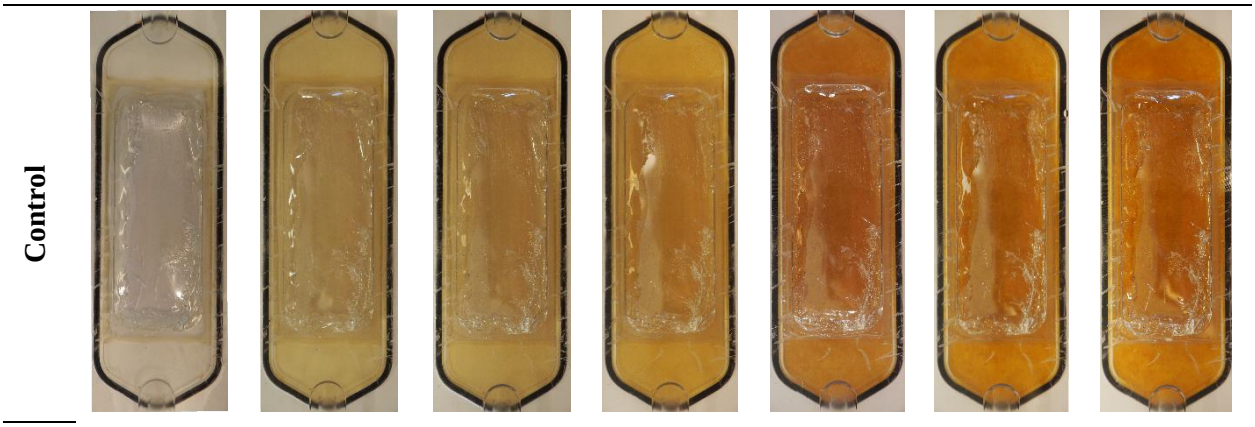

	Day 0	Day 1	Day 2	Day 9	Day 21	Day 28	Day 34
GA(M)	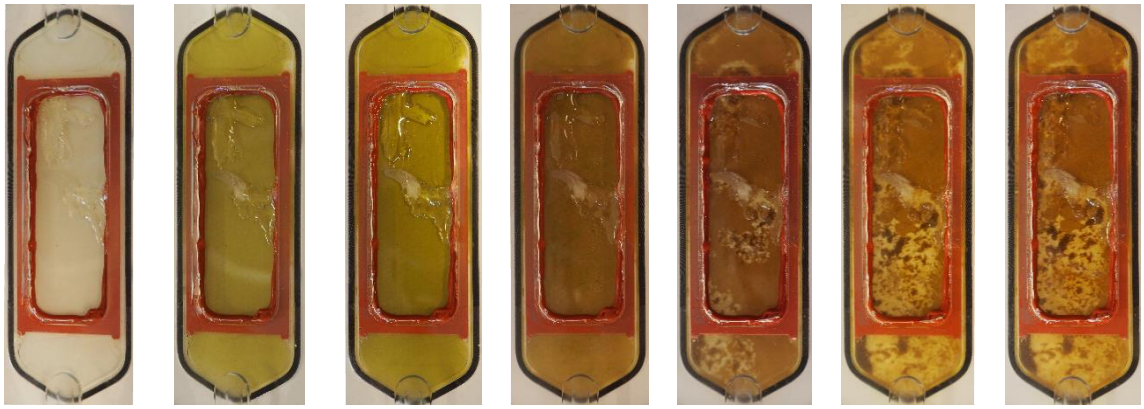						
	Day 0	Day 1	Day 2	Day 9	Day 21	Day 28	Day 34
GA(H)	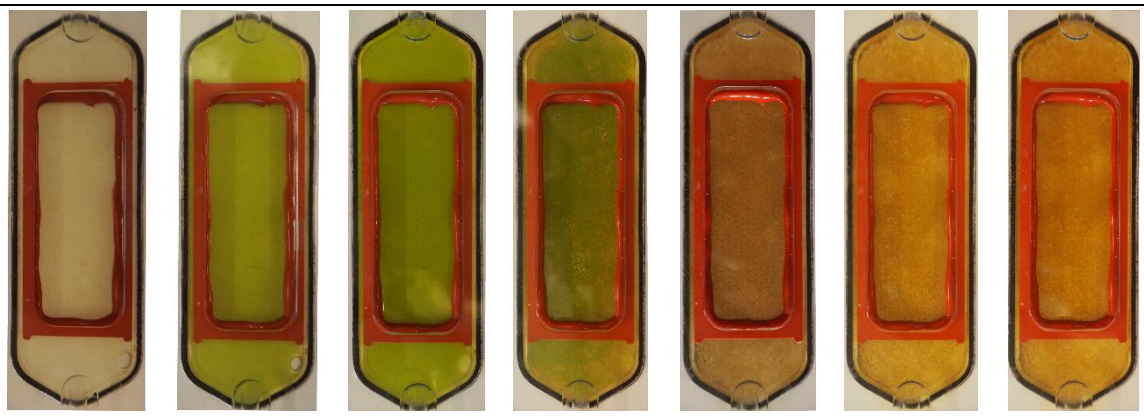						
	Day 0	Day 1	Day 2	Day 9	Day 21	Day 28	Day 34
DI(M)	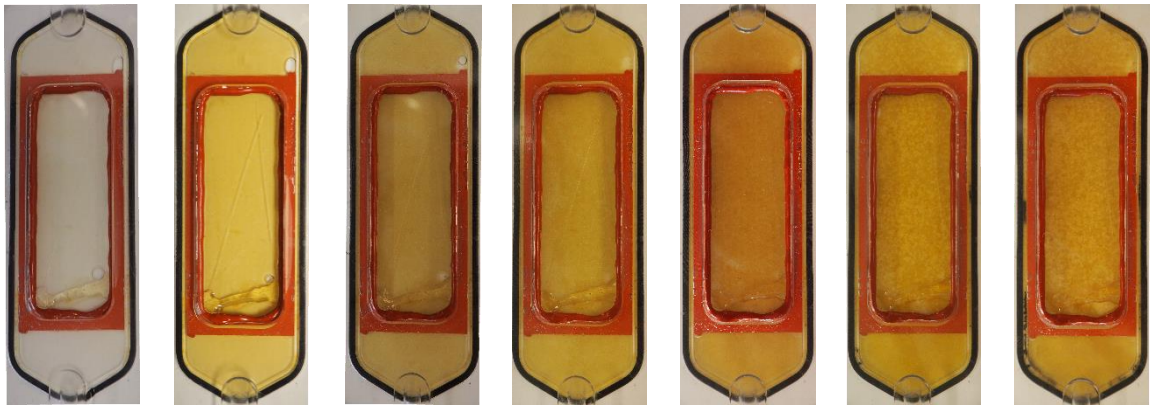						
	Day 0	Day 1	Day 2	Day 9	Day 21	Day 28	Day 34

Figure S4. Photos of the fouled membranes in the Stage II

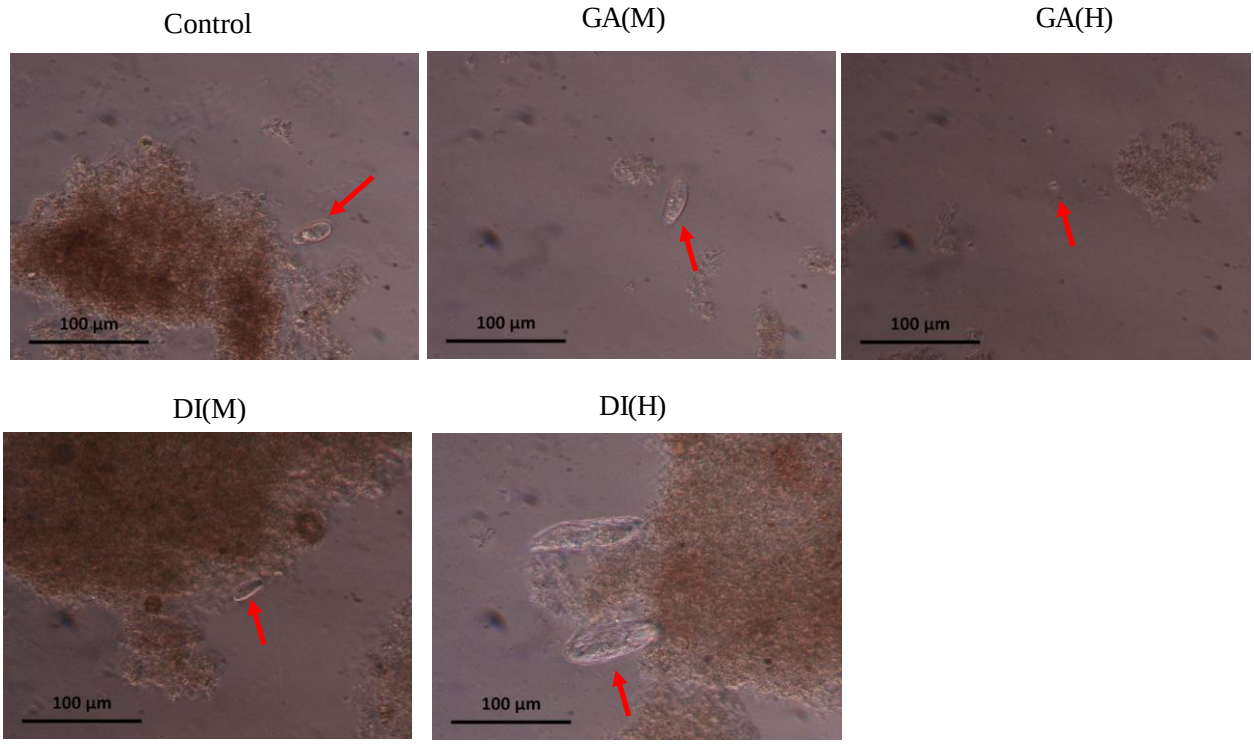

Figure S5. Microscopic observations of the eukaryotes in the biofilm layer on the membranes in the Stage II